A Statistical Approach to Quantum Mechanics*

M. Creutz and B. Freedman

Physics Department, Brookhaven National Laboratory, Upton, New York 11973

Received November 13, 1980

A Monte Carlo method is used to evaluate the Euclidean version of Feynman's sum over particle histories. Following Feynman's treatment, individual paths are defined on a discrete (imaginary) time lattice with periodic boundary conditions. On each lattice site, a continuous position variable x_i specifies the spacial location of the particle. Using a modified Metropolis algorithm, the low-lying energy eigenvalues, $|\psi_0(x)|^2$, the propagator, and the effective potential for the anharmonic oscillator are computed, in good agreement with theory. For a deep double-well potential, instantons were found in our computer simulations appearing as multi-kink configurations on the lattice.

I. Introduction

Feynman's path integral formulation of quantum mechanics reveals a deep connection between classical statistical mechanics and quantum theory. Indeed, in an imaginary time formalism the Feynman integral is mathematically equivalent to a partition function. Using this analogy, particle physicists have recently employed a well-known technique of statistical mechanics in using Monte Carlo simulation to study gauge field theories [1, 2]. The simulations are a means of numerical evaluation of the path integrals. This has yielded new non-perturbative insight into the behavior of quantized Yang–Mills fields.

A gauge system is a rather complicated quantum theory with many degrees of freedom. This masks the connection between a Euclidean Monte Carlo treatment and a more traditional Hilbert space formulation of quantum mechanics. In this paper we search for such connections by studying a considerably simpler model, a one-degree-of-freedom Schrödinger system. We will see how Monte Carlo methods can provide information on the ground and first excited states of this problem. We do not advocate these methods for accuracy, rather we hope they may lead to better understanding of the workings of the Monte Carlo method. Furthermore, these methods are rather easily generalizable to systems with many degrees of freedom.

This paper is organized as follows. In Section II we review the Feynman formalism and present the formulas we will use in our numerical studies. Section III presents and

427

justifies the Monte Carlo method for evaluation of these path integrals. Section IV contains some numerical results obtained from the simple harmonic and anharmonic oscillators. Section V is a brief conclusion and in the Appendixes we treat more carefully some technical details.

II. The Path Integral

In this section we will study the similarities between quantum theory and statistical mechanics. Our fundamental tool will be the Euclidean (imaginary time) version of Feynman's sum over histories [3]:

$$Z_{fi} = \langle x_f \mid e^{-HT/\hbar} \mid x_i \rangle$$

$$\sim \int [dx]\, e^{-S[x]/\hbar}, \tag{2.1}$$

Both representations of Z require explanation:

The vectors $\mid x_i \rangle$ and $\mid x_f \rangle$ in Eq. (2.1) are position eigenstates, H is the Hamiltonian operator for a spinless particle of mass m_0 moving in a potential, where

$$H(P, Q) = \tfrac{1}{2}P^2/m_0 + V(Q), \tag{2.2}$$

and T is a positive number. Equation (2.1) is of interest because, if we expand in a complete set of energy eigenstates,

$$H \mid n \rangle = E_n \mid n \rangle \tag{2.3}$$

then

$$Z_{fi} = \sum_n e^{-E_n T/\hbar} \langle x_f \mid n \rangle \langle n \mid x_i \rangle. \tag{2.4}$$

Thus, at large T the leading term in this expression gives us the energy and wave-function of the lowest-lying energy eigenstate.

The second form for Z must also be explained. The Euclidean action is given by

$$S = \int_0^T d\tau \left[\tfrac{1}{2} m_0 \left[\frac{dx}{d\tau} \right]^2 + V(x) \right], \tag{2.5}$$

where $\tau = it$ (t is real time), and $\int [dx]$ denotes integration over all functions $x(\tau)$ obeying the boundary conditions

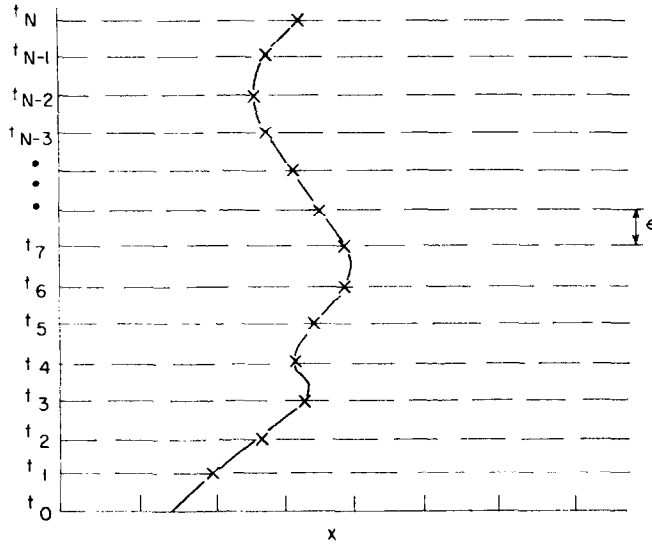$$x(0) = x_i, \tag{2.6a}$$

and

$$x(T) = x_f. \tag{2.6b}$$

FIG. 1. Making time discrete to label paths.

The original version of Feynman's Path Integral is of the form

$$Z(x_f, x_i) = \sum_{\text{paths}} \exp iS_m/\hbar, \qquad (2.7)$$

where the sum is over all world lines that connect the initial and final points, and S_m is the Minkowski space action for a particular path. A precise definition of the "sum over all paths" must be provided before Eq. (2.7) becomes useful. One way to proceed is to introduce a time lattice, so that various paths can be labelled simply (Fig. 1). Making the time axis discrete, we adopt the following notation:

$$x(t_j) = x_j \qquad (j = 0, 1,..., N), \qquad (2.8)$$

where $-\infty < x_j < \infty$ for all sites j, and

$$t_{j+1} - t_j = \epsilon, \qquad (2.9)$$

where ϵ is the spacing between adjacent time slices. Expression (2.7) is a sum of rapidly oscillating phases. By continuing to imaginary time each path will be weighed by an ordinary damped exponential factor, making it easier to distinguish important paths from unimportant paths. This is our Euclidean Path Integral given in Eq. (2.1). The integration measure is now well defined and is given by

$$Z_{fi} \sim \int_{-\infty}^{+\infty} \prod_{j=1}^{N-1} dx_j \exp\left(-\frac{1}{\hbar} S[x_j]\right) \qquad (N \to \infty), \qquad (2.10)$$

where $T = Na$. The action for a discrete time lattice is just

$$S = \sum_{j=1}^{N} a \left[\frac{1}{2} m_0 \frac{[x_{j+1} - x_j]^2}{a} + V(x_j) \right],$$ (2.11)

where $a = i\epsilon$. We use the boundary conditions $x_0 = x_i$ and $x_N = x_f$. The continuum limit is recovered by letting $N \to \infty$ and $a \to 0$, keeping T fixed. For later use we define the trace of Z_{fi}

$$Z = \int dx_i \, dx_f \, \delta(x_f - x_i) \, Z_{fi} \, .$$

Equation (2.10) is identical to the partition function for a statistical mechanics problem. We have a one-dimensional lattice with sites labeled by index j. On each site there is a variable x_j, which takes on continuous values as given by (2.8). The action couples nearest-neighbor variables x_j and x_{j+1}, and the integral $\int \prod_{j=1}^{N-1} dx_j$ is really a sum over all possible lattice configurations. The Boltzmann factor is just

$$e^{-1/\hbar S[x]},$$ (2.12)

where $\hbar = $ temperature, and the Euclidean action, (2.11), is the classical Hamiltonian for a system with N degrees of freedom.

In statistical mechanics the temperature is a measure of the statistical fluctuations in a system, while in quantum mechanics $\hbar$ is a measure of the quantum fluctuations (through the uncertainty principle). In quantum mechanics, the $\hbar \to 0$ limit picks out classical physics. In particular, as $\hbar \to 0$ the classical trajectory for a particle moving in a potential $V(x)$ becomes the only path that contributes to the transition amplitude Z_{fi}, fluctuations are completely suppressed. As T approaches zero for a statistical system, fluctuations are frozen out. These points allow for a one-to-one correspondence between doing quantum mechanics in imaginary time and statistical mechanics on a real crystal lattice.

Since Z is a partition function we can also define a free energy for our lattice, namely

$$Z = e^{-\beta F} \qquad (F = \text{free energy}),$$ (2.13a)

or

$$F = -\frac{1}{\beta} \ln Z,$$ (2.13b)

where $\beta = 1/\hbar$. Because F is an extensive quantity, it is useful to define a free energy density f, where $F = f \cdot T$, and T is the volume of our (time) crystal. Equation (2.13) now becomes

$$f = \frac{-1}{\beta T} \ln Z,$$ (2.14)

which as $T \to \infty$ yields

$$f = E_0 . \tag{2.15}$$

As in statistical mechanics, it is useful to measure correlation functions, which are given formally by

$$\Gamma^{(n)} = \text{Tr } e^{-HT/\hbar} x(\tau_1) \, x(\tau_2) \cdots x(\tau_n)/Z, \tag{2.16a}$$

where

$$Z = \int_{-\infty}^{+\infty} dx \langle x \mid e^{-HT/\hbar} \mid x \rangle = \text{Tr } e^{-HT/\hbar}. \tag{2.16b}$$

In quantum theory the $\Gamma^{(n)}$ are called n-point propagator functions. We can write Eq. (2.16) in a compact form by defining

$$Z(J) = \text{Tr } e^{-T/\hbar[H + \Sigma_i^n J_i x_i]}, \tag{2.17}$$

where J_i is an external c-number current ($\delta J_i/\delta J_k = \delta_{ik}$). Then we have

$$\Gamma^{(m)} = \frac{\delta}{\delta J_1} \frac{\delta}{\delta J_m} Z(J) \bigg|_{J=0}$$

From the logarithm of Z we obtain the connected n-point functions

$$\Gamma_c^{(n)} = \frac{\delta}{\delta J_1} \cdots \frac{\delta}{\delta J_n} \ln Z(J) \bigg|_{J=0} . \tag{2.18}$$

For example,

$$\Gamma_c^{(2)} = \langle x(\tau_1) \, x(\tau_2) \rangle - \langle x(\tau_1) \rangle \langle x(\tau_2) \rangle, \tag{2.19}$$

where we have adopted the notation

$$\langle \hat{A} \rangle = \text{Tr}(e^{-HT/\hbar} \hat{A})/\text{Tr}(e^{-HT/\hbar}) \tag{2.20}$$

for any operator $\hat{A}$. In terms of the functional (path) integral, (2.20) is equivalent to the expression:

$$\frac{\int_{-\infty}^{+\infty} \prod_{i=1}^{N} dx_i \, A(x_1, x_2, ..., x_n) \, e^{-1/\hbar S[x]}}{\int_{-\infty}^{+\infty} \prod_i dx_i \, e^{-1/\hbar S[x]}}, \tag{2.21}$$

where now $A(x_1, ..., x_n)$ is just a normal function of the x's. The propagators $\Gamma^{(n)}$ for a spin-system in statistical mechanics are the correlation functions

$$\Gamma_{\text{SM}}^{(n)} = \langle S_1 S_2 \cdots S_n \rangle, \tag{2.22}$$

where the S_i are spin variables at sites $\{i\}$ in the crystal.

In the limit $T \to \infty$, we recover the expectation values of our operators in the quantum theory:

$$\hat{A} = \frac{\sum_n e^{-E_n T/\hbar} \langle n \mid \hat{A} \mid n \rangle}{\sum_n e^{-E_n T}}$$

$$= \langle 0 \mid \hat{A} \mid 0 \rangle, \qquad \text{as} \quad T \to \infty. \tag{2.23}$$

In this case, the two-point fuuction $\Gamma_c^{(2)}$ becomes

$$\lim_{T \to \infty} \Gamma_c^{(2)} = \langle 0 \mid x(0)\, x(\tau) \mid 0 \rangle - \langle 0 \mid x \mid 0 \rangle^2$$

$$= \sum_{n \neq 0} e^{-1/\hbar (E_n - E_0)\tau} |\langle 0 \mid x \mid n \rangle|^2. \tag{2.24}$$

We can find the energy gap between E_1 and E_0 by taking the large t limit in Eq. (2.24). Choosing $\tau' > \tau \to \infty$, we see that

$$\frac{\Gamma_c^{(2)}(\tau')}{\Gamma_c^{(2)}(\tau)} = e^{-(E_1 - E_0)(\tau' - \tau)/S}, \tag{2.25a}$$

or

$$\frac{1}{\hbar}(E_1 - E_0) = \lim_{T \to \infty} \left(\frac{-1}{\Delta t} \ln[\Gamma_c^{(2)}(\tau + \Delta\tau)/\Gamma^{(2)}(\tau)] \right). \tag{2.25b}$$

To determine the lowest energy eigenvalue, E_0 is in principle easy, since we know that

$$E_0 = \langle 0 \mid H \mid 0 \rangle = \lim_{T \to \infty} [\mathrm{Tr}(e^{-HT/\hbar} H)/\mathrm{Tr}\, e^{-HT/\hbar}]$$

$$= \lim_{T \to \infty} \frac{-1}{T} \frac{\partial}{\partial(\hbar^{-1})} \ln Z. \tag{2.26a}$$

Using the path integral representation for Z, Eq. (2.26a) becomes

$$E_0 = \lim_{T \to \infty} \frac{-1}{T} \frac{\partial}{\partial(\hbar^{-1})} \ln \int [dx]\, e^{-1/\hbar S[x]}. \tag{2.26b}$$

Unfortunately, the expectation value of the action, $\langle S \rangle$, diverges like $1/a$ for small lattice spacing. For any potential $V(x)$, the velocity-dependent part of $\langle S \rangle$ behaves in the following way:

$$\lim_{a \to 0} \frac{\langle (x_{i+1} - x_i)^2 \rangle}{a^2} = \frac{\hbar}{m_0} \cdot \frac{1}{a} + O(1) \cdots, \tag{2.27}$$

Although a mean velocity can be defined, no mean-square velocity exists at any point. In other words, the important paths for a quantum-mechanical particle are non-

differentiable! Although these paths are very irregular, one possible remedy is to define the expectation of v^2 following Feynman and Hibbs [3]

$$\langle v_i{}^2 \rangle = - \frac{\langle (x_{i+1} - x_i)(x_i - x_{i-1}) \rangle}{a^2}. \tag{2.28}$$

The expectation value in Eq. (2.28) is perfectly well behaved when $a \to 0$. Eq. (2.28) is a split-point definition for $v_i{}^2$ and allows us to calculate E_0 for our system. Operators local in time, in contrast, have a nice continuum limit as $a \to 0$; no redefinition is necessary. An alternative procedure is to use the virial theorem to calculate the kinetic energy

$$\tfrac{1}{2} M_0 \langle v_i{}^2 \rangle = \tfrac{1}{2} \langle x \cdot V'(x) \rangle, \tag{2.29}$$

The ground-state energy is thus given by the formula:

$$E_0 = \lim_{T \to \infty} \left(\int [dx]\, e^{-1/\hbar S[x]} [\tfrac{1}{2} x V'(x) + V(x)] \Big/ \int [dx]\, e^{-1/\hbar S[x]} \right). \tag{2.30}$$

The ultimate goal is to evaluate the integrals in the partition function. For most potentials, however, analytic solutions simply do not exist. Furthermore, we must do N integrations, where N becomes infinite as $a \to 0$. In the next section, we describe a numerical method for calculating the expectation values of operators [as in (2.21)] motivated, in part, by statistical physics.

III. EVALUATING PATH INTEGRALS

In this section we describe a technique for performing the sum "over paths" of the Feynman Integral [4]. This approach is based on the Monte Carlo method of Metropolis *et al.* [5].

Let us begin by defining the expectation value of any operator $\hat{A}$ for a finite time interval T as

$$\langle \hat{A} \rangle = \sum_k A(\mathbf{x}_k) \exp[-S(\mathbf{x}_k)] \Big/ \sum_k \exp[-S(\mathbf{x}_k)], \tag{3.1}$$

where $\mathbf{x}_k$ denotes a configuration (or path) of the system. Each configuration depends on N dynamical variables $\{x_i\}$ which give the position of the particle at each timeslice $\{t_i\}$. The action for a configuration $\mathbf{x}_k = (x_1^{(k)}, x_2^{(k)} \cdots x_N^{(k)})$ is given by

$$S(\mathbf{x}_k) = \sum_{i=1}^{N} a\mathscr{L}(x_i^{(k)}, x_{i+1}^{(k)}), \tag{3.2}$$

where the Lagrangian couples nearest-neighbor variables and $T = Na$. In statistical mechanics, Eq. (3.1) corresponds to the canonical ensemble average of an operator $\hat{A}$

for a system of N classical particles described by a Hamiltonian, $H_N \leftrightarrow S$. Noting that x_i takes on one value from a continuous set of points

$$-\infty < x_i < \infty, \tag{3.3}$$

we can write Eq. (3.1) more explicitly

$$\langle A \rangle = \int \mathscr{D}\mathbf{x} A(\mathbf{x}) \exp[-S(\mathbf{x})] \Big/ \int \mathscr{D}\mathbf{x} \exp[-S(\mathbf{x})]. \tag{3.4}$$

The measure used in the functional integral is

$$\int \mathscr{D}\mathbf{x} = \int_{-\infty}^{+\infty} \prod_{i=1}^{N} dx_i. \tag{3.5}$$

The basic goal of the Monte Carlo method is to evaluate the "phase-space" sums or integrals in Eqs. (3.1), (3.4) numerically. We approximate an integral $\int f(\mathbf{x}) \mathscr{D}\mathbf{x}$ by a sum with a finite number of terms $\sum_\nu f(\mathbf{x}_\nu) \varDelta \mathbf{x}_\nu$. Note, however, that the integrand $\exp[-S(\mathbf{x}_\nu)]$ will vary over many orders of magnitude for moderately large time intervals T. Thus, a simple random sampling of points $\mathbf{x}_\nu$ would be impractical for purposes of real computation. The Monte Carlo method introduced by Metropolis is based on the idea of "importance sampling." Here the phase-space points $\mathbf{x}_\nu$ in Eq. (3.4) are not selected completely at random, but are more densely distributed in that region of phase space giving the dominant contributions to the integrals. Motivated by statistical mechanics, we wish to choose states $\mathbf{x}_\nu$ according to the Boltzman distribution

$$P^{\text{eq}}(\mathbf{x}_\nu) \mathscr{D}\mathbf{x} = \frac{\exp[-S(\mathbf{x}_\nu)] \mathscr{D}\mathbf{x}}{\int \mathscr{D}\mathbf{x} \exp[-S(\mathbf{x})]}. \tag{3.6}$$

Then the Monte Carlo estimate $\bar{A}$ for the quantity $\langle A \rangle$ simply reduces to an arithmetic average

$$\bar{A} = \frac{1}{M} \sum_{\nu=1}^{M} A(\mathbf{x}_\nu), \tag{3.7}$$

where M is the total number of states generated in the Monte Carlo sequence.

The realization of "importance sampling" is possible using a Markov process to generate the M configurations $\{\mathbf{x}_\nu\}$ in Eq. (3.7) [6]. This process is constructed so that in the limit where M becomes infinite the probability of occurrence of configuration $\mathbf{x}_\nu$ in the Markov chain is given by Eq. (3.6). It is useful to review the basic features of the Markov process since it figures so prominently in things to come.

A Markov chain is described by an $N \times N$ matrix W $(N \leqslant \infty)$ with entries $W_{ij} \geqslant 0$ satisfying the condition

$$\sum W_{ij} = 1 \tag{3.8}$$

for all i. The idea is that W_{ij} should represent the probability that a system, currently in state s_i makes a transition into a state s_j in one Markov step, which we loosely refer to as one unit of time. Here the indices i and j label the possible configurations of the system. We can extend this definition to include continuous state spaces by defining a transition probability density, $W(x, x')$, for $\mathbf{x} \to \mathbf{x}'$ satisfying

$$W(x, x') \geq 0, \tag{3.9a}$$

and

$$\int dx'\, W(x, x') = 1 \qquad \text{(for all } x\text{).} \tag{3.9b}$$

In a two step process from x to x' (or s_i to s_j) the system must pass through some intermediate state x_1. The probability of a transition from x to x' in two steps in a Markov chain is given by

$$W^{(2)}(x, x') = \int dx_1\, W(x, x_1)\, W(x_1, x'). \tag{3.10}$$

For a discrete system this would correspond to matrix multiplication. Similarly for an n-step process, we have

$$W^{(n)}(x, x') = \int dx_1 \cdots \int dx_{n-1} W(x, x_1)\, W(x_1, x_2) \cdots W(x_{n-1}, x')$$
$$= \int dx_\alpha\, W^{(n-1)}(x, x_\alpha)\, W(x_\alpha, x'). \tag{3.11}$$

The long time behavior of the system can be approached by studying the limiting properties of $W^{(n)}$ as $n \to \infty$. Using properties (3.9) of the transition "matrix" it is possible to show that

$$\lim_{n \to \infty} W^{(n)}(x, x') = P^*(x'), \tag{3.12}$$

for all x. In the large n limit, the transition probability function is independent of the initial configuration and is given by $P^*(x)$. For a discrete system, the $\lim_{n \to \infty} W_{ij}$ exists and is a matrix with identical rows. For the interested reader the proof of Eq. (3.12) can be found in Appendix B. In Eq. (3.11), taking $n \to \infty$ shows that $P^*(x)$ is stationary in the sense that:

$$P^*(x') = \int dx_\alpha\, P^*(x_\alpha)\, W(x_\alpha, x'). \tag{3.13}$$

In other words, P^* is a left eigenvector of M with an eigenvalue of unity. From Eq. (3.9), $P^*(x)$ also satisfies the condition of a probability distribution

$$P^*(x) \geq 0 \qquad \text{(for all } x\text{),} \tag{3.14a}$$

and

$$\int dx'\, P^*(x') = 1. \qquad (3.14b)$$

It is an easy matter to show P^* is unique. Let P be another set of probabilities satisfying (3.13), and (3.14); then

$$P(x') = \int dx_\alpha\, P(x_\alpha)\, W(x_\alpha, x'). \qquad (3.15)$$

Iterating Eq. (3.15) n times,

$$P(x') = \int dx_\alpha\, P(x_\alpha)\, W^{(n)}(x_\alpha, x'). \qquad (3.16)$$

Allowing $n \to \infty$ in Eq. (3.16), we find

$$
\begin{aligned}
P(x') &= \lim_{n\to\infty} \int dx_\alpha\, P(x_\alpha)\, W^{(n)}(x_\alpha, x') \\
&= \int dx_\alpha\, P(x_\alpha)\, P^*(x') \\
&= P^*(x'), \qquad \text{for all } x'.
\end{aligned}
\qquad (3.17)
$$

Therefore, P^* is the unique fixed point of the Markov process in the limit the chain becomes infinite.

To sumarize, we wish to construct $W(x, x')$ to satisfy

$$W(x, x') > 0 \qquad (\text{if } P(x) > 0 \quad \text{and} \quad P(x') > 0), \qquad (3.18a)$$

$$\int dx'\, W(x, x') = 1, \qquad (3.18b)$$

$$P^{\mathrm{eq}}(x') = \int dx\, P^{\mathrm{eq}}(x)\, W(x. x'), \qquad (3.18c)$$

where P^{eq} is the same probability appearing in (3.6). Applying W in (3.18) n times to an initial ensemble E_i produces the following chain

$$E_i \xrightarrow{W} E_i^{(1)} \xrightarrow{W} E_i^{(2)} \xrightarrow{W} \cdots \xrightarrow{W} E_i^{(n)}. \qquad (3.19)$$

Completely independent of our starting configuration E_i, we know that

$$\lim_{n\to\infty} E_i^{(n)} = E^*, \qquad (3.20)$$

where E^* is the equilibrium ensemble with probabilities given by $\{P^{\mathrm{eq}}\}$. It is useful

to think of $\hat{W}$ as an evolution operator in "ensemble space." A point in this space is defined by the probabilities of our ensemble, that is

$$E = (P_1{}^E, P_2{}^E, ..., P_j{}^E, ...). \tag{3.21}$$

We can even go so far as to define a norm in this space

$$\| E - E' \| = \sum_{i=1}^{N} | P_i - P'_i |, \tag{3.22a}$$

which in the continuum limit becomes

$$\| E - E' \| = \int dx \, | P(x) - P'(x)|. \tag{3.22b}$$

Figure 2 shows a Markov process for two different starting configurations E_A and E_B. The time needed to reach E^* will in general be different for these two cases. If our initial ensemble has a configuration close to E^*, convergence will be rapid. It pays to make a good guess. There are ways of selecting a reasonable starting E_i which we shall describe later in this section.

We now turn to the task of explicitly constructing a transition probability $W(x, x')$ from the requirements of Eq. (3.18). Note that these requirements do not specify W
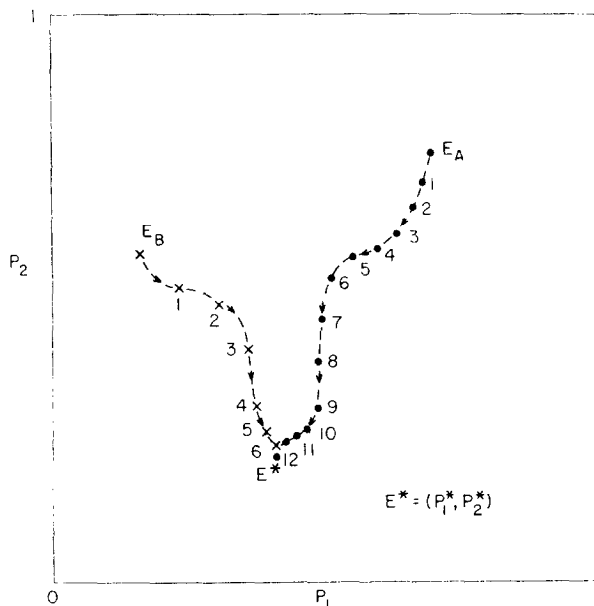

FIG. 2. Approaching equilibrium from different directions.

uniquely. A simple choice by which Eq. (3.18) is fulfilled is provided by the detailed balance condition

$$\frac{W(\mathbf{x}, \mathbf{x}')}{W(\mathbf{x}', \mathbf{x})} = \frac{P^{\mathrm{eq}}(\mathbf{x}')}{P^{\mathrm{eq}}(\mathbf{x})} .$$ (3.23)

Using (3.23) in Equation (3.18c) satisfies the requirement that P^{eq} is an eigenvactor of $\hat{W}$, since

$$
\begin{aligned}
P^{\mathrm{eq}}(x') &= \int dx\, P^{\mathrm{eq}}(x)\, W(x, x') \\
&= \int dx\, P^{\mathrm{eq}}(x)\, W(x', x)\, \frac{P^{\mathrm{eq}}(x')}{P^{\mathrm{eq}}(x)} \\
&= \int dx\, W(x, x')\, P^{\mathrm{eq}}(x') \\
&= P^{\mathrm{eq}}(x').
\end{aligned}
$$ (3.24)

Equation (3.23) still does not specify $W(x, x')$ uniquely. Considerations of efficiency and computational feasibility eventually dictate its form. In our work we have followed the rather common procedure of probing the lattice variables one at a time, so that $E^{(i)}$ and $E^{(i+1)}$ differ, at most, in the va x')of a single variable x_j. Here we use the term "probing" to mean the effect of $W(x \to x')$ on the lattice at a certain time in the chain. For our procedure W is really a single step stransition probability (W_s). The detailed balance condition for W_s is extremely simple. Using Eq. (3.6) for P^{eq} and keeping all but one variable, x_j, fixed, we find

$$\frac{W_s(\mathbf{x}, \mathbf{x}')}{W_s(\mathbf{x}', \mathbf{x})} = \frac{e^{-S(x'_j)}}{e^{-S(x_j)}} ,$$ (3.25)

where $S(x_j)$ is the action associated with x_j, and depends only on x_j and its nearest neighbors. The Markov process is defined by probing successively all the statistical variables of the lattice many times. One complete sweep through the lattice is referred to as one Monte Carlo iteration. When all the spins have been analyzed, we proceed to a new iteration. The matrix defining the Markov process for a Monte Carlo iteration is given by

$$W^{(N)} = W_s(x'_N, x_N)\, W_s(x'_{N-1}, x_{N-1}) \cdots W_s(x'_2, x_2)\, W_s(x'_1, x_1).$$ (3.26)

This still leaves open the detailed form of the transition probability $W_s(x'_i, x_i)$. The most intuitive way to satisfy Eq. (3.25) is to pick

$$W_s(x_j, x'_j) \sim e^{-S(x'_j)}.$$ (3.27)

Thus, the transition probability for a single step is proportional to the Boltzmann factor for x'_j. This method is referred to as the "Heat Bath" algorithm [1, 2, 7]. It has the feature that the variable being probed is always changed according to (3.27). Histori-

cally, the first method for solving (3.25) was introduced by Metropolis *et al.* [5], and is called the "Metropolis algorithm" (what else). It differs from the Heat Bath method in several important ways. The simplest form of W_s in the Metropolis method is given by

$$W_s(x_j, x'_j) = \frac{1}{N_0}\left\{1 \cdot \theta[S(x_j) - S(x'_j)] + \exp[-\Delta S(x'_j, x_j)] \theta[S(x'_j) - S(x_j)]\right.$$

$$\left. + \int dx'[1 - \exp(-\Delta S(x'_j, x_j)] \theta[S(x') - S(x_j)] \delta(x'_j - x_j)\right\}, \quad (3.28)$$

where $\Delta S(x', x) = S(x') - S(x)$, and N_0 is the volume of the configuration manifold. Equation (3.28) looks incredibly complicated when compared with Heat Bath, however, it is by far the simpler of the two to implement in a real calculation.

To understand the simplicity of this algorithm, let us analyze (3.28) in some detail: The method of Metropolis begins by choosing randomly a new value x'_j with uniform probability. If the action is lowered by the replacement of x_j with x'_j, the variable at site j is set to this new value. If $\Delta S \geq 0$; then a random number r with uniform distribution between 0 and 1 is generated and the variable is changed to x'_j only if $\exp(-\Delta S) > r$. Otherwise, the lattice variable retains its previous value, x_j. The next site is then probed in exactly the same way, and so on through the lattice. It is a simple exercise to check Eq. (3.28) satisfies (3.18a), (3.18b). To see that it also satisfies detailed balance let us choose x and x' so that $S(x') < S(x)$. Then according to Eq. (3.28), $W_s(x, x') = 1$ and $W_s(x', x) = e^{-\Delta S(x,x')}$. Conversely, if $S(x') > S(x)$, then $W_s(x, x') = e^{-\Delta S(x',x)}$ and $W_s(x', x) = 1$. The Metropolis algorithm reduces the distance of an ensemble from equilibrium by less per iteration than the heat bath; however, computational speed often more than compensates for this.

We have described only two methods for implementing detailed balance, there are certainly more. For example, it is often useful if the new state is rather close to the old one; in the Metropolis algorithm this is simply achieved by introducing a parameter Δ. Then $x_j \xrightarrow{W_s} x'_j$, where $x_j - \Delta \leq x'_j \leq x_j + \Delta$. This is extremely useful when the configuration space is large but the action highly peaked. The previous method would take a long time to change a configuration, since most of the new x's would be rejected by the condition $e^{-\Delta S} > r$. Another modification can be made by increasing the number of Metropolis hits per site. This improves convergence to equilibrium, since a configuration change is more likely to take place:

$$x_j \xrightarrow{W_s} x_j^{(1)} \xrightarrow{W_s} x_j^{(2)} \to \cdots \xrightarrow{W_s} x_j^{(\bar{n})}, \quad (3.29)$$

where x'_j is set equal to $x_j^{(\bar{n})}$ before proceeding to the next lattice site. Therefore, the algorithm we use is characterized by two additional parameters Δ and $\bar{n}$, and satisfies, of course, Eqs. (3.18).

Finally, there is the matter of choosing an initial configuration close to E^*. This clearly requires some prior knowledge of what the equilibrium ensemble looks like. In general this is known for only limiting cases of our system: at high temperatures ($\hbar \gg 1$) we expect the lattice to be random, while for low temperature ($\hbar \to 0$) classical

configurations of the action will dominate. Starting in either of these two configurations, we can then iterate systematically to $\hbar = 1$ (hopefully, both will agree!). For simple systems an educated guess will work almost as well, and saves a lot of computing time.

Usually we test for equilibrium by measuring some expectation value as a function of iteration time. We observe that average values of local operators settle down before we see the same numerical convergence in long range correlation functions. The notion of being in equilibrium is somewhat ill defined because the average value of one operator may "stabilize" before that of another. Our proof of a fixed point (E^*) rested on taking $n \to \infty$, making the Markov chain infinitely long. For finite n, deviations from E^* will produce inaccuracies, the size of which can not be foretold. Different operators will be affected by this deviation from E^* in different ways. In practice we always end-up working with finite chains, and so it is up to us to minimize the effects of $\| E^{(n)} - E^* \|$ on the operator we are measuring by adjusting E_i, Δ, and $\bar{n}$.

IV. NUMERICAL STUDIES

Our work has many features of an experiment. We work on a one-dimensional crystal, at a temperature equal to $\hbar$, which comes into thermal equilibrium after a relaxation time. Once in equilibrium we measure the free energy, correlation functions, anything (in principle) we want. Our crystal has N degrees of freedom $(x_1, x_2, ..., x_N)$, where each x_j is located at site j on the lattice, and

$$\infty \leqslant x_j \leqslant \infty, \tag{4.1}$$

$$x_0 = x_N. \tag{4.2}$$

The dynamics of our crystal is governed by the action

$$S = a \sum_{i=1}^{N} \frac{1}{2} M_0 \frac{(x_{i+1} - x_i)^2}{a^2} + V(x_i), \tag{4.3}$$

Here we consider the anharmonic oscillator potential

$$V(x_i) = \tfrac{1}{2}\mu^2 x_i^2 + \lambda x_i^4. \tag{4.4}$$

In our computer simulations, we worked on lattices with

$$N \sim 10^2 \text{ to } 10^3 \text{ sites} \tag{4.5}$$

Our choice for N, and a, was motivated by two considerations: (1) the lattice size, a, must be small enough to approximate the continuum limit; (2) Na must be sufficiently

large to isolate the ground-state properties of our model. Defining $T_E = 2\pi\hbar/E_0$ we typically picked N and a so that

$$a/T_E \sim 1/10 \text{ to } 1/20, \tag{4.6a}$$

$$Na/T_E \sim 3 \text{ to } 10. \tag{4.6b}$$

Another problem is the size of statistical fluctuations in our crystal. For an operator $f = \sum_{i=1}^{N} f_i$, the relative fluctuation of f about its average $\bar{f}$ is measured by

$$\Delta_f = \frac{(\overline{\Delta f^2})^{1/2}}{|\bar{f}|} \sim N^{-1/2} \tag{4.7}$$

where $\Delta f = f - \bar{f}$, and N is the number of lattice sites. To compute $\bar{f}$ we average over N_E "identical" crystals according to Eq. (3.7).

The time needed to reach equilibrium in units of Metropolis iterations was strongly dependent on lattice spacing but for moderately large a was typically found to be

$$N_t \sim 10 \text{ to } 50 \text{ iterations} \tag{4.8}$$

depending on our choice for the initial lattice configuration. Using the Metropolis algorithm, we then generated N_E lattice configurations. To keep members of our ensemble statistically independent of one another, 3–5 Monte Carlo iterations were made between lattice measurements. The Metropolis algorithm used in our computer simulations had

$$\Delta \sim 2\sqrt{a} \tag{4.9}$$

and

$$\bar{n} \sim 5 \text{ to } 10. \tag{4.10}$$

In most of our experiments $N_E \sim 10^2$ gave reasonably small statistical fluctuations. Once in equilibrium, averages of moments and correlation functions

$$\overline{x_i^2},\ \overline{x_i^4},\ \overline{x_i x_{i+m}},... \tag{4.11}$$

were measured. But from Eq. (3.7), we also know that Eq. (4.11) is equivalent to

$$\langle \hat{x}^p \rangle = \overline{x_i^p}, \tag{4.12a}$$

and

$$\langle \hat{x}(0)\ \hat{x}(\tau) \rangle = \overline{x_i x_{i+m}}, \tag{4.12b}$$

where $\tau = ma$.

Using Eqs. (4.11), (4.12), we were able to measure the low-lying states of the energy spectrum, E_0 and E_1. These eigenvalues were computed from the following formulas:

$$E_0 = u^2 \langle x^2 \rangle + 3\lambda \langle x^4 \rangle \quad \text{(virial theorem)}, \tag{4.13}$$
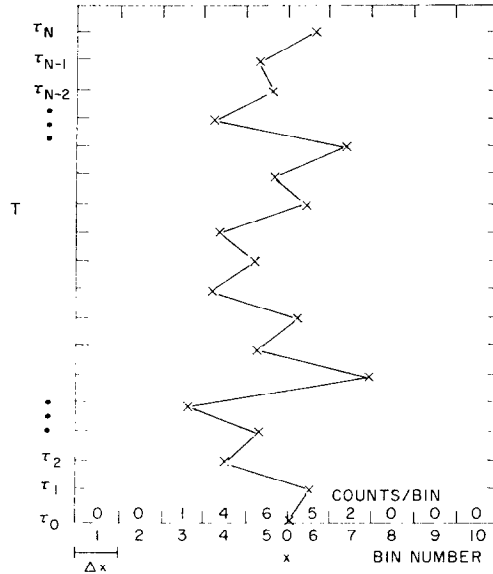
FIG. 3. Binning the coordinates to study the ground-state wavefunction.

and

$$E_1 = \frac{-1}{\Delta\tau} \ln \left[\frac{\langle x(0)\, x(\tau + \Delta\tau)\rangle}{\langle x(0)\, x(\tau)\rangle} \right] + E_0, \qquad \tau \to \infty. \tag{4.14}$$

Likewise, we found the probability for finding a particle in the interval $(x + \Delta x, x - \Delta x)$ from our data. Dividing the "x-axis" into bins of size Δx, we know that (see (A.26)):

$$|\psi_0(x)|^2 = \frac{1}{\Delta x} \sum_{\{i\}}^{N_{\mathrm{TOT}}} \theta(\Delta x - |x_i - x|) \Big/ \sum_{\{i\}}^{N_{\mathrm{TOT}}} 1, \tag{4.15}$$

where Δx is small, $N_{\mathrm{TOT}} = N \cdot N_E \to \infty$, and the sum is over our Monte Carlo configurations. Equation (4.15) is pictured in Fig. 3, We chose Δx so a sufficient number of our events were recorded in each bin. Fluctuations in the jth bin behaved like $\sim 1/\sqrt{n_j}$, where n_j was the number of times a trajectory passed through $x_j \pm \Delta x$. N_{TOT} was an extremely large number in our simulations $\sim 10^4$ to 10^6.

A typical quantum trajectory from our Monte Carlo of the harmonic oscillator is shown in Fig. 4. The values of the potential parameters were $m = 1.0$, $\mu^2 = 1.0$, $\lambda = 0$. We worked on a 1000 site lattice with $a = 0.1$. Figure 5 shows the probability density for the ground state of the harmonic oscillator. Averaging over 300 Monte Carlo iterations, with $N = 1000$ and $a = 1.0$, we found the Monte Carlo points agreed with theory
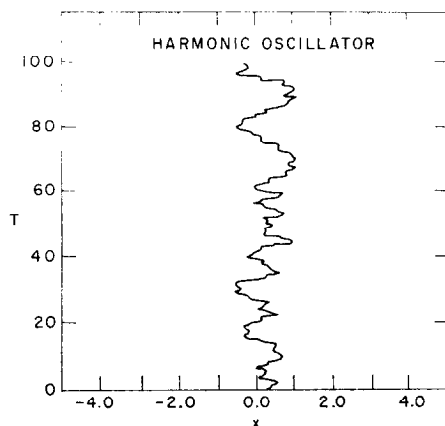
$$|\psi_0(x)|^2 = 0.59 \exp -(1.1)\, x^2 \tag{4.16}$$

FIG. 4.   A typical quantum trajectory for the harmonic oscillator.

within statistical fluctuations $\sim 2\%$. Eq. (4.16) is the result one obtains for the discrete harmonic oscillator on a lattice this size and is derived in Appendix C. This is to be compared with the continuum answer $(a \to 0)$

$$| \psi_0(x)|^2 = \frac{1}{\sqrt{\pi}} \exp - x^2. \qquad (4.17)$$

In Fig. 5 we denote the points of our simulation by x's, the lattice theory prediction by a dotted line, and the continuum result by a solid line. The potential $V(x)$ and M_0 were the same as before.

A semi-log plot of the correlation function for the harmonic oscillator vs "time" separation t is shown in Fig. 6. The parameters used in this case were $M_0 = 0.5$,
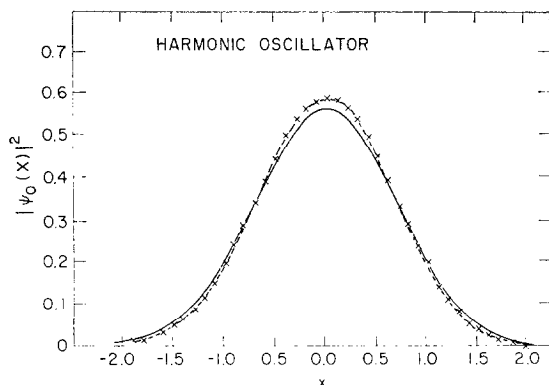
FIG. 5.   The ground-state probability density for the harmonic oscillator. The crosses are the Monte Carlo results, the dashed curve represents the discrete theory, and the solid curve gives the continuum theory.
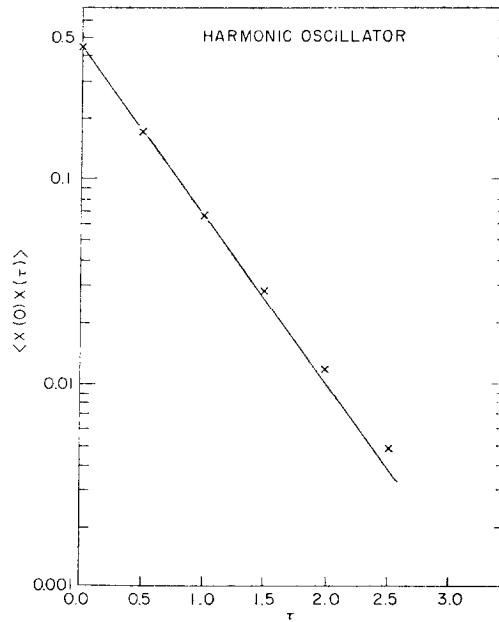
FIG. 6.   The correlation between coordinates as a function of their time separation for the harmonic oscillator.

$\mu^2 = 2.0$, $\lambda = 0$, with $N = 51$ and $a = 0.5$. The x's are our Monte Carlo points while the solid line is the theoretical prediction. The straight line in Fig. 6 indicates that only $\langle 0 \mid \hat{x} \mid 1 \rangle$ is non-zero. This is correct for a harmonic oscillator since $\hat{x} \sim \hat{a} - \hat{a}^+$. From Fig. 6 we find $\langle x^2 \rangle = 0.45$, $E_1 - E_0 = 1.98$, and $\Delta_E = 0.13$ for $N_E = 100$. These numbers should be compared to the theoretical values: $\langle x^2 \rangle = 0.447$, $E_1 - E_0 = 1.975$, $\Delta_E = 0.11$. In the limit $a \to 0$, $\langle x^2 \rangle = 0.5$ and $E_1 - E_0 = 2.0$.

Figure 7 shows samples of quantum paths generated by Monte Carlo for the anharmonic oscillator. It is convenient to rewrite the potential (4.4) as

$$V(x) = \lambda(x^2 - f^2), \tag{4.18}$$

where the zeros of the potential occur at the classical minima, $x = \pm\sqrt{f^2}$. This amounts to rescaling S by an additive constant. For our computations we selected to keep $\lambda = 1$, and vary f^2. In Figs. 7a–c we choose $M_0 = 0.5$, $a = 1.0$, and $N = 50$. We waited ~40 iterations before recording the $\{x$'s$\}$ in each case. The tunneling density was found to decrease rapidly as we varied f^2 from 0 to 2. Figure 7c shows a typical multi-kink configuration [8]. The dotted lines denote the positions of the classical minima of $V(x)$ at $x = \sqrt{f^2}$. Figure 8 is a graph of the ground-state probability $\mid \psi_0(x)\mid^2$ vs x for the value of $f^2 = 2.0$. Using the parameters $M_0 = 0.5$, $a = 0.25$, $N = 200$, we averaged over 100 Monte Carlo iterations. The small number of tunnelings at large f^2 is reflected in the low probability around the origin in Fig. 8.
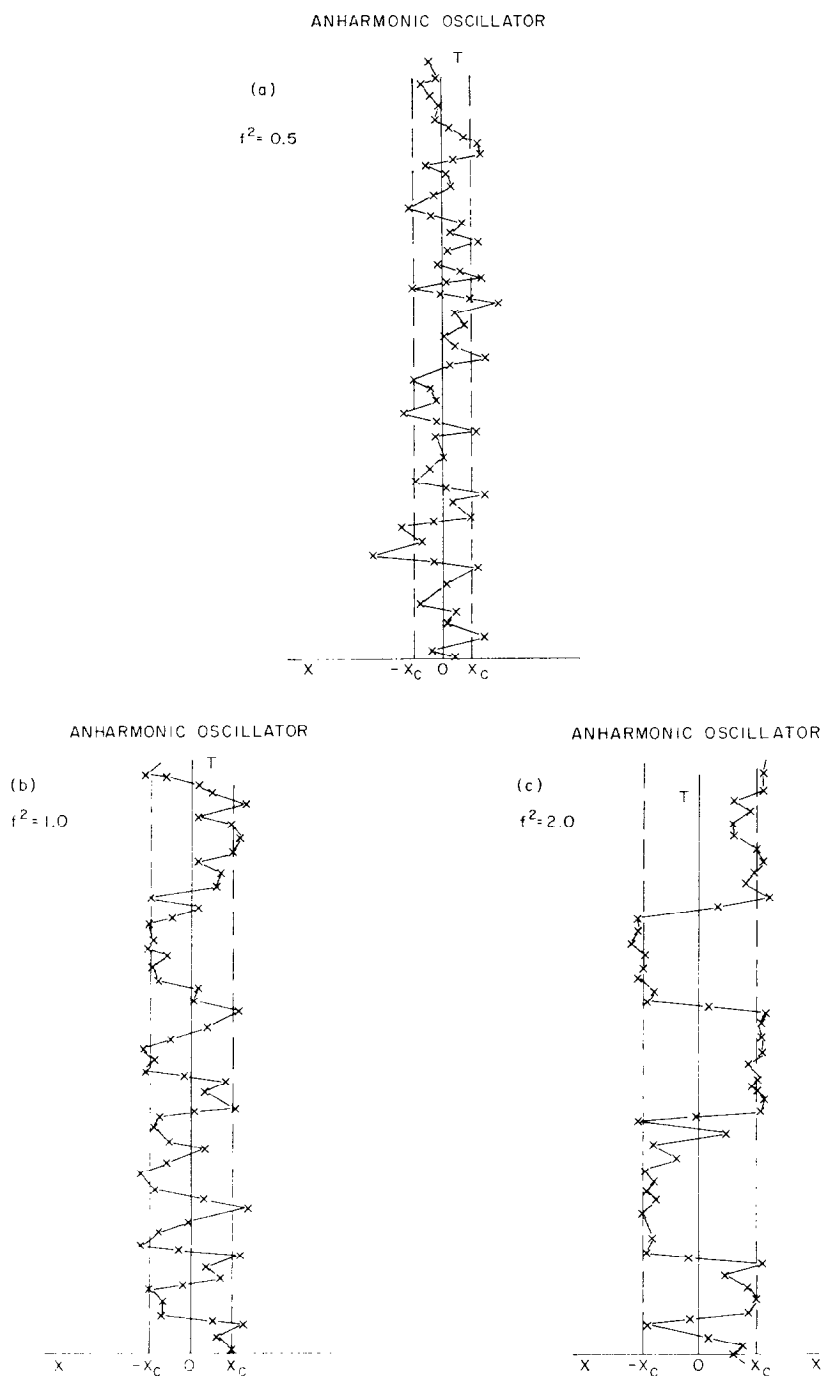
ANHARMONIC OSCILLATOR

(a)

$f^2 = 0.5$

ANHARMONIC OSCILLATOR

(b)

$f^2 = 1.0$

ANHARMONIC OSCILLATOR

(c)

$f^2 = 2.0$

FIG. 7. Typical paths for the anharmonic oscillator for (a) $f^2 = 0.5$, (b) $f^2 = 1.0$ and (c) $f^2 = 2.0$.
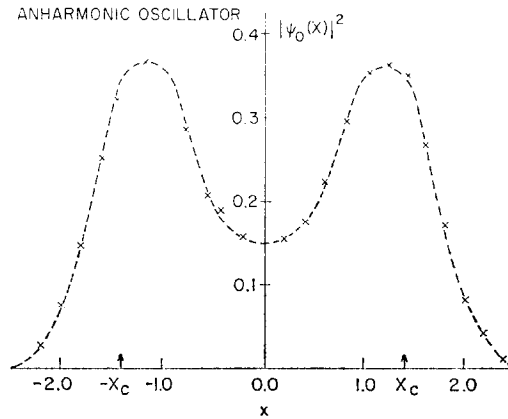
FIG. 8. The ground-state probability distribution for an anharmonic oscillator.

Figure 9 is a semi-log plot of $\langle x(0)x(\tau) \rangle$ vs τ for different choices of $\bar{n}$. Again Again $f^2 = 2.0$ was picked, with $M_0 = 0.5$, $a = 0.25$, and $N = 303$. We performed an ensemble average consisting of 10 Monte Carlo iterations. Since we use periodic boundary conditions, we are actually averaging over 3,030 values of $x(0)x(\tau)$ for each value of τ. We clearly must limit correlations of $t/a \ll N/2$. Increasing $\bar{n}$ improved the Monte Carlo estimate of the correlation function with $\bar{n} \sim 15$ giving the best results for this case. Choosing $\bar{n}$ too large will slow down the Monte Carlo simulation,
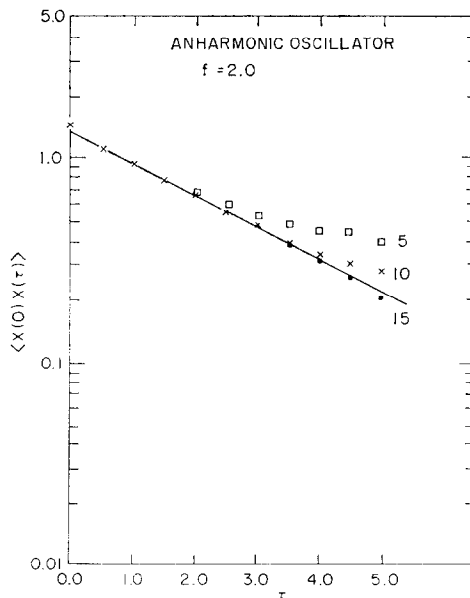

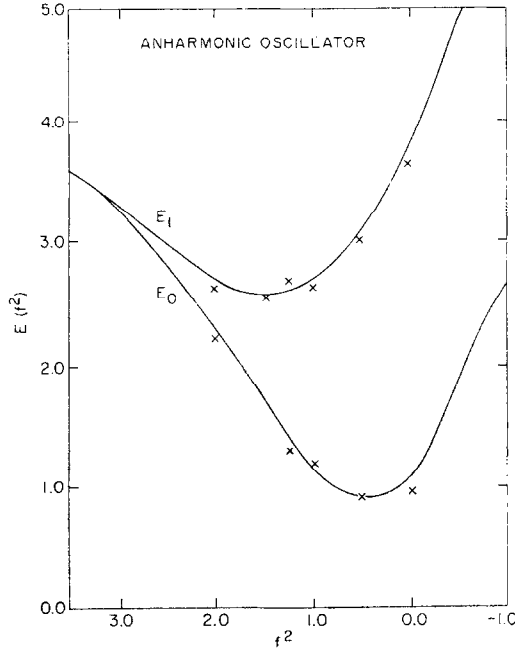FIG. 9.   Correlation versus time separation for the anharmonic oscillator.

FIG. 10. The first two energy levels of the anharmonic oscillator as functions of the parameter f^2.

so picking an optimal value for $\bar{n}$ is necessary. Figure 10 is a plot of the low-lying energy levels vs f^2. The solid lines are the known results from the continuum theory [9], the x's are the Monte Carlo predictions. Unfortunately, the energy eigenvalues, $\{E_n(f^2)\}$, are not available for comparison when N and a are finite, non-zero, numbers.

Coupling an external c-number source J to the site variables $\{x_i\}$ we studied the response of the crystal to an external current. The new action for the lattice is given by

$$S \rightarrow S' = S + J \sum_{i=1}^{N} x_i , \tag{4.19}$$

where S is the old action. Since the new interaction breaks reflection symmetry, the expectation value $\langle n \rangle_J = x_J$ will not automatically vanish. Figure 11 shows x_J vs J for the harmonic oscillator. It is straightforward to prove that when $\lambda = 0$,

$$J = \mu^2 x_J \tag{4.20}$$

for all a. In Fig. 11 we selected $M_0 = 0.5$, $\mu\lambda = 2.0$, $N = 51$, and $a = 0.1$. The solid line is Eq. (4.20), the x's are the results of our computer simulations. This experiment was repeated for the anharmonic oscillator, with $M_0 = 0.5$, $f^2 = 2.0$, $N = 303$, and $a = 0.25$. The Monte Carlo curve is the dotted line in Fig. 12, the x's are data points
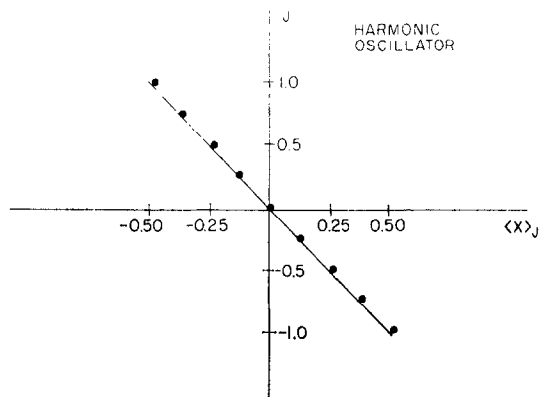
CREUTZ AND FREEDMAN

FIG. 11. The expectation x_0 as a function of applied source J for the harmonic oscillator.

from our computer simulation. The solid line in Fig. 12 is a plot of the classical x_J obtained by solving

$$J = -\frac{\delta V(x)}{\delta x}, \tag{4.21}$$

and $V(x) = (x^2 - f^2)^2$.

Using Figs. 11, 12 we can define a new function $J(x_J)$ for these two cases. Integrating $J(x_J)$, we obtain a new function called the effective potential [10]:
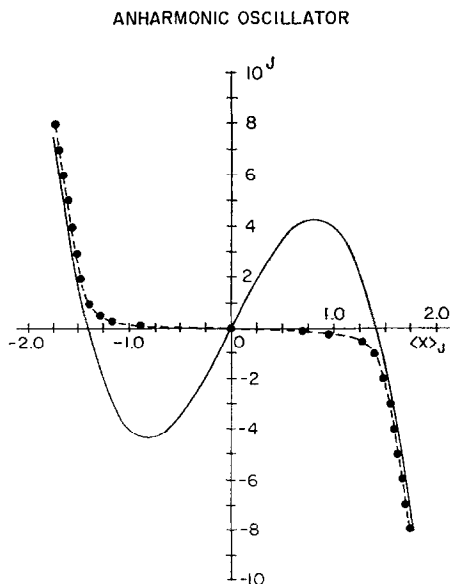
$$V_R(x_J) = \int_{x_J} dx' \, J(x'). \tag{4.22}$$

ANHARMONIC OSCILLATOR

FIG. 12. The expectation x_0 as a function of J for the anharmonic oscillator.

HARMONIC OSCILLATOR
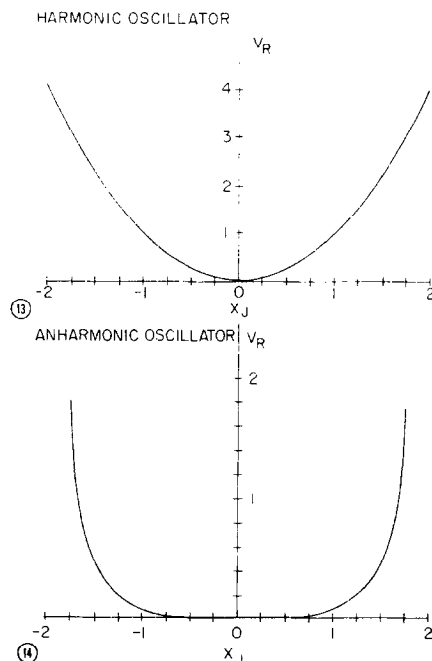

ANHARMONIC OSCILLATOR

FIG. 13.   The effective potential for the harmonic oscillator.
FIG. 14.   The effective potential for the anharmonic oscillator.

$V_R(x_J)$ displays the true symmetries of the quantum theory—for this reason it can be thought of as the renormalized potential of the Hamiltonian. Figure 13 shows $V_R(x_J)$ vs x_J for the harmonic oscillator. $V_R(x_J)$ is identical to the classical potential $V(x)$. Figure 14 shows the effective potential for the anharmonic oscillator. The effective potential in Fig. 14 has a single minimum at $x_J = 0$. This is not surprising since we know spontaneous symmetry breaking does not occur in quantum mechanics. Nevertheless, it is amusing that we can compute $V_R(x_J)$ using Monte Carlo techniques.

We can also isolate classical solutions [9] to the Euclidean equations of motion by sending $\hbar \rightarrow 0$. For the anharmonic oscillator we can accomplish the same thing by making the barrier height larger ($f^2 \rightarrow \infty$). We are specifically interested in finite action solutions which contribute to the transition probabilities

$$\langle x_c \mid e^{-\hat{H}T} \mid -x_c \rangle, \tag{4.23a}$$

$$\langle -x_c \mid e^{-\hat{H}T} \mid x_c \rangle, \tag{4.23b}$$

where $x_c = \sqrt{f^2}$. These tunneling solutions will dominate over quantum fluctuations $\sim O(\hbar)$. To find a single kink we must impose antiperiodic boundary conditions

$$x(N + i) = -x(i), \tag{4.24}$$

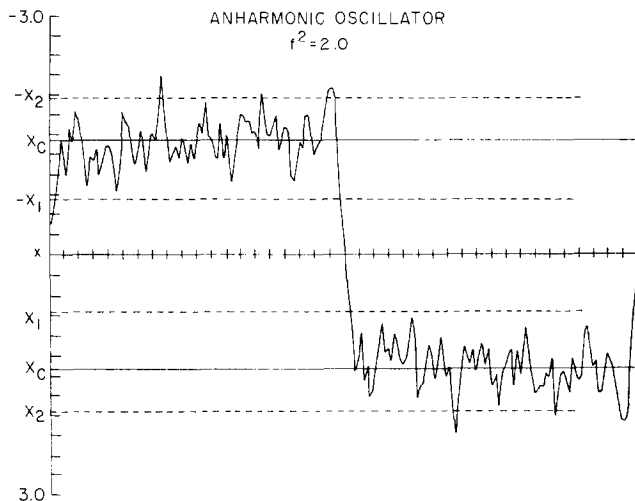and $f^2 \gg 1$. Figure 15 shows a single kink configuration for $M_0 = 0.5$, $f^2 = 2.0$,

FIG. 15.   A single kink configuration for the anharmonic oscillator with antiperiodic boundary conditions.

$N = 200$, and $a = 0.25$. The classical minima are denoted by $\pm x_c$, and the classical turning points are at $\pm x_1$ and $\pm x_2$. Figure 16 is a plot of $x(t)$ vs t, where $x(t)$ is a solution of $m\ddot{x} = V'(x)$ satisfying

$$x(-T/2) = -x_c,\tag{4.25a}$$

$$x(+T/2) = +x_c,\tag{4.25b}$$

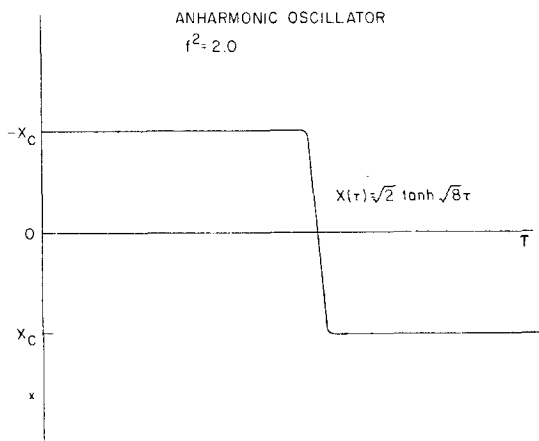where T is assumed to be large. These figures are in remarkable agreement.

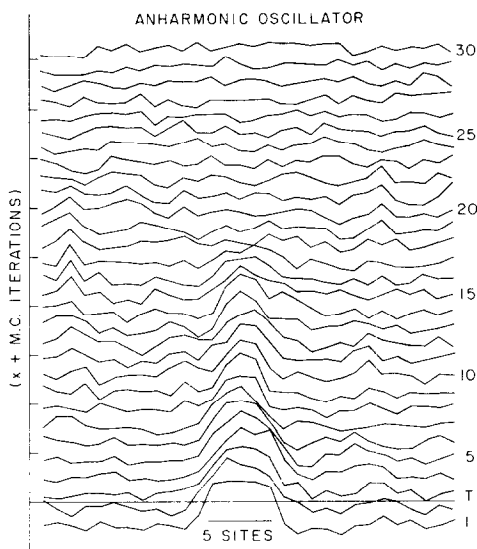FIG. 16.   The classical tunnelling solution for imaginary time.

FIG. 17.   The annihilation of two kinks.

Figure 17 shows the Monte Carlo evolution of a kink pair under conditions where the equilibrium kink density is small. We worked on a 30 site lattice, $a = 0.5$, with symmetric boundary conditions. Our crystal was initialized with a two-kink configuration. After each pass through the lattice the new $\{x_i\}$'s were plotted, this was done 30 times. The potential was chosen to have

$$V(0) - V(\pm x_c) = 4, \tag{4.26}$$

where $x_c = 2.0$. With these parameters, the equilibrium density of kinks in our crystal satisfied

$$\rho_K^{\text{eq}} \cdot T \ll 1. \tag{4.27}$$

Note how the two initial kinks attract and annihilate after roughly 18 iterations. It is well known that an n-kink state can decay into a smaller number of kinks, $n \to n'$, so long as $n + n' =$ even. The simulation is consistent with this result. The amount of time for this to happen depended on the relative size of the quantum fluctuations to the kink–kink separation in our lattice.

V. CONCLUSION

In this paper we have shown how to apply Monte Carlo methods to the study of simple quantum systems. The method quite easily gives information about the ground state of a particle in arbitrary potential. The most serious shortcoming of the method

appears to lie in the study of levels beyond the first two. As the technique relies on an imaginary time formulation, the contribution of higher states are exponentially suppressed and therefore difficult to extract.

The main advantage of the method as applied to quantum mechanics is the almost trivial generalization to more degrees of freedom by adding more variables to the simulation. This has been dramatically illustrated by the successes of Monte Carlo studies of gauge theories. In going to a field theory, the time slicing used here generalizes to a space–time lattice. In addition to serving as a means of definition of the path integral, this lattice also provides an ultraviolet cutoff. This non-perturbative regulator gives control over the divergences which are rampant in quantum field theory.

The effective potential discussed in the last section will show its true value in higher dimensional field theories. Historically, it was introduced to study the spontaneous breaking of symmetries of the Hamiltonian. In addition, parameters characterizing the renormalized effective potential can be used in defining a renormalization scheme.

Finally we remark that Monte Carlo simulations in principle include all possible field configurations. If some particular type of excitations, i.e., topological, are physically important, they should be seen upon careful examination of the simulated configurations. Thus we saw the "kink" configurations giving rise to tunneling phenomena in the anharmonic oscillator.

APPENDIX A: FUNDAMENTALS

Let us begin by considering a quantum mechanical system with one degree of freedom [12]. Let $Q_H(t)$ be the position operator at time t in the Heisenberg picture:

$$Q_H(t) = e^{iHt} Q_s e^{-iHt} \qquad (\hbar = 1), \qquad (A.1)$$

where $Q_s = Q_H(0)$.

The eigenstates of $Q_H(t)$ are defined by the condition

$$Q_H(t) \mid q, t \rangle_H = q \mid q, t \rangle_H \qquad (A.2)$$

or $Q_s e^{-iHT} \mid q, t \rangle_H = q e^{-iHt} \mid q, t \rangle_H$, where q is the position coordinate at time t (it is just a c-number!). Now we define the states $\{\mid q \rangle\}$ as the eigenstates of Q_s with eigenvalue q:

$$Q_s \mid q \rangle = q \mid q \rangle. \qquad (A.3)$$

Then we have

$$\mid q, t \rangle_H = e^{iHt} \mid q \rangle. \qquad (A.4)$$

An especially interesting quantity in quantum theory is the transition matrix $_H\langle q't' \mid q, t \rangle_H$ which is the probability amplitude for the state prepared at t with the

coordinate q to become the state of coordinate q' at time t'. According to (A.4) this is given by

$$_H\langle q', t' \mid q, t \rangle_H = \langle q' \mid e^{-iH(t'-t)} \mid q \rangle. \tag{A.5}$$

We can imagine partitioning the time interval $t' - t$ into N segments, so that each segment goes to zero as $N \to \infty$. For simplicity, we shall divide the interval into N equal segments of duration Δ, such that

$$(t' - t)/N = \Delta. \tag{A.6}$$

Upon writing

$$e^{iH(t'-t)} = e^{iH(t'-t_{n-1})}e^{iH(t_{n-1}-t_{n-2})} \cdots e^{iH(t_1-t)} \tag{A.7}$$

and inserting complete sets of eigenstates of Q_s between the factors, we obtain

$$\langle q' \mid e^{-iH(t'-t)} \mid q \rangle = \int dq_1 \cdots \int dq_{n-1} \langle q' \mid e^{-iH\Delta} \mid q_{n-1} \rangle$$
$$\times \langle q_{n-1} \mid e^{-iH\Delta} \mid q_{n-2} \rangle \cdots \langle q_1 \mid e^{-iH\Delta} \mid q \rangle. \tag{A.8}$$

We consider a Hamiltonian of the form $H(P, Q)$, where

$$H(P, Q) = \tfrac{1}{2}P^2 + V(Q). \tag{A.9}$$

Now for sufficiently small Δ we can factor $\langle q' \mid e^{-iH\Delta} \mid q \rangle$ as follows:

$$\langle q' \mid e^{-iH\Delta} \mid q \rangle = \langle q' \mid T \mid q \rangle + O(\Delta^2),...,$$

where

$$T = e^{-i/2 V(Q)\Delta}e^{-i/2P^2\Delta}e^{-i/2V(Q)\Delta}. \tag{A.10}$$

This operator is called the transfer matrix [11]. We can evaluate (A.10) by inserting a complete set of momentum eigenstates $\{\mid p \rangle\}$ between the factors, where

$$\hat{p} \mid p \rangle = p \mid p \rangle, \tag{A.11a}$$

$$\langle q \mid p \rangle = e^{ipq}. \tag{A.11b}$$

It is a straightforward calculation to show

$$\langle q' \mid T \mid q \rangle = \int \frac{dp}{2\pi} e^{ip \cdot (q'-q)}e^{-i\Delta H(p \cdot q, q)}, \tag{A.12}$$

where $H(p; q, q')$ is an ordinary function of the form

$$H(p; q, q') = \tfrac{1}{2}p^2 + \tfrac{1}{2}V(q) + \tfrac{1}{2}V(q'). \tag{A.13}$$

When $q' \to q$, Eq. (A.13) is just the classical expression for the Hamiltonian.

Finally, substituting Eq. (A.12) into (A.8), we obtain

$$\langle q' \mid e^{-iH(t'-t)} \mid q \rangle = \int \prod_{i=1}^{N} \frac{dp_i}{2\pi} \int \prod_{i=1}^{N-1} dq_i \exp i \sum_{i=1}^{N} \Delta \left\{ p_i \frac{(q_i - q_{i-1}}{\Delta} \right.$$

$$\left. - H(p_i ; q_i , q_{i-1}) \right\}, \tag{A.14}$$

where $N \to \infty$, $\Delta \to 0$, such that $t' - t = Na$ remains fixed. Since H is quadratic in p, we can perform all the momentum integrations analytically.

$$\langle q' \mid e^{-iH(t'-t)} \mid q \rangle = \sqrt{2\pi \Delta} \int \prod_{i=1}^{N-1} dq_i \exp i \sum_{i=1}^{N} \Delta \left\{ \left(\frac{q_i - q_{i-1}}{\Delta} \right)^2 \middle/ 2 - V(q_i + q_{i-1}/2 \right\}, \tag{A.15}$$

where we imposed the boundary condition $q_n = q'$, and $q_0 = q$. Equation (A.15) is the form first written down by Feynman. Writing the velocity $\dot{q}$ as

$$\dot{q} = \left(\frac{q_i - q_{i-1}}{\Delta} \right) \qquad (\Delta \to 0), \tag{A.16}$$

Equation (A.15) becomes

$$\langle q' \mid e^{-iHT} \mid q \rangle = \int [dq] \exp i \int_0^T dt \, \mathcal{L}(\dot{q}, q), \tag{A.17}$$

$\mathcal{L}(\dot{q}, q) = \frac{1}{2}\dot{q}^2 - V(q)$.

For finite spacing Δ, the path integral is directly related to the transfer matrix given in Eq. (A.10). The Hamiltonian for the discrete system is formally given by the operator

$$H_s = (i/\Delta) \ln T. \tag{A.18}$$

In the limit Δ goes to zero, H_s becomes the original Hamiltonian in Eq. (A.9),

$$\lim_{\Delta \to 0} H_s = H. \tag{A.19}$$

Since the transfer matrix is a unitary operator, it has a spectral decomposition of the form

$$T = \sum_n \mid n \rangle \, e^{-iE_n\Delta} \langle n \mid, \tag{A.20}$$

where the $\{\mid n \rangle\}$ are eigenstates of H_s with corresponding iegenvalues E_n. The transfer matrix or the path integral gives the same information about the quantum theory as

solving Schrödinger's equation, namely the spectrum of states, wavefunctions, and all the rest. In the continuum limit

$$T = \exp - i \, \Delta[H + O(\Delta)], \tag{A.21}$$

which we identify as the time-evolution operator for an infinitesimal step, Δ.

The Schrödinger picture is recovered by observing that the wavefunction is the amplitude for finding a particle at x at time t regardless of how it got there. Therefore, the transition amplitude $Z(x, t, x_0, t_0)$ is really a wavefunction. In fact, $Z(x, t, x_0, t_0)$ gives us more information than is required, since it also tells us that the particle started out at x_0 at time t_0. Using the rule for combining amplitudes, and identifying $\psi(x, t) - Z(x, t, 0, 0)$, we find that ψ must satisfy

$$\psi(x', t') = \int dx \, Z(x', t', x, t) \, \psi(x, t). \tag{A.22}$$

Choosing $t' - t = \epsilon$ to be infinitesimal, Eq. (A.22) becomes

$$\psi(x', t') = \psi(x', t) - i\epsilon H \psi(x', t), \tag{A.23a}$$

where we used the fact

$$\begin{aligned}
Z(x', t + \epsilon, x, t) &= \langle x' \mid T \mid x \rangle \\
&= = \langle x' \mid 1 - i\epsilon H \mid x \rangle \\
&= \delta(x' - x) - i\epsilon H(x)\delta(x' - x).
\end{aligned}$$

Equation (A.23) is just the Schrödinger equation:

$$i\dot\psi(x, t) = H(x) \cdot \psi(x, t). \tag{A.23b}$$

In Feynman's version of quantum mechanics, the probability for finding a particle between $x - \Delta x$ and $x + \Delta x$ is just a time average over transition amplitudes (Fig. 18):

$$P(x; T) = \frac{1}{T} \int_0^T dt' \int_{x-\Delta x}^{x+\Delta x} dx' \frac{Z(x_f, T; x', t') \, Z(x', t', x_i, 0)}{Z(x_f, T; x_i, 0)}. \tag{A.24}$$

Note, Eq. (A.24) keeps track of the number of times the particle passes through x with resolution Δx during the time interval T. Let us assume Δx is so small, that we can replace the integral over x' by its value at x. Continuing (2.24) to imaginary time, and using Eq. (2.4) for Z_{fi}, the time integration can be performed, yielding:

$$\begin{aligned}
P(x, T) = \Delta x \, Z_{fi}^{-1}(T) \Bigg\{ &\sum_n \mid \phi_n(x)\mid^2 \phi_n^*(x_i) \, \phi_n(x_f) \, e^{-E_n T} \\
&+ \sum_{n \neq n'} \phi_{n'}^*(x_i) \, \phi_n(x_f) \, \phi_n^*(x) \, \phi_{n'}(x) \left(\frac{e^{-E_{n'} T} - e^{-E_n T}}{(E_{n'} - E_n) \, T} \right) \Bigg\}
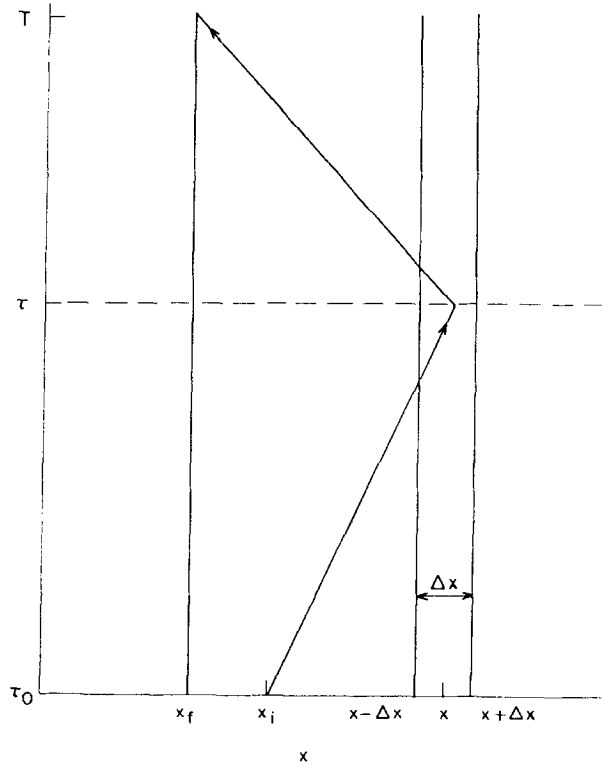\end{aligned} \tag{A.25}$$

CREUTZ AND FREEDMAN

FIG. 18.   Graphical interpretation of Eq. (A.24).

Taking $T \to \infty$, we obtain

$$\frac{P(x, T)}{\Delta x} = |\phi_0(x)|^2 + O\left(\frac{1}{\Delta E_{\mathrm{MIN}} T}\right), \qquad (A.26)$$

where $\Delta E_{\mathrm{MIN}} = E_1 - E_0$. For $T \gg 1/E_1 - E_0$, we isolate the ground-state probability density, $\lim_{T \to \infty} P(x, T) = P_0(x)$. Note, all dependence on x_i, x_f, and T has disappeared, due to the normalization factor Z_{fi}^{-1} in (A.24):

$$\lim_{T \to \infty} Z_{fi}(T) = \phi_0^*(x_i)\, \phi_0(x_f)\, e^{-E_0 T}.$$

APPENDIX B: More About Markov Chains [6]

Let W_{ij} be the transition probability matrix for a finite system with N states. In the Markov chain the nth step transition matrix is defined by

$$W_{ij}^{(n)} = \sum W_{i\alpha}^{(n-1)} W_{\alpha j}, \qquad (B.1)$$

where $\sum_j W_{ij} = 1$, and $W_{ij} > 0$ if P_1 and P_j are greater then zero. Then the following is true:

$$\lim_{n \to \infty} W^{(n)} = -\Pi \tag{B.2}$$

exists, where Π is a matrix with identical rows and satisfying the same properties as W.

The proof that $W_{ij}^{(\infty)}$ is independent of the initial state i is completely straightforward. Assume first that $n = 1$, so that $W_{ij} \geq \epsilon > 0$ for each i, j. Let $m_j(n) = \min_i W_{ij}^{(n)}$ denote the smallest element in the jth column of $W^{(n)}$, and similarly let $M_j(n)$ be the largest element. Rewriting Eq. (B.1) as

$$W_{ij}^{(n)} = \sum_k W_{ik} W_{kj}^{(n-1)}, \tag{B.3}$$

then

$$W_{ij}^{(n)} \geq \sum_k W_{ik} m_j(n-1) = m_j(n-1). \tag{B.4}$$

Both (B.1) and (B.3) express $W^{(n)}$ as the matrix multiplication of W n-times. Since Eq. (B.4) holds for each i, it holds for the minimum, and so the column minima increase with n,

$$m_j(n) \geq m_j(n-1).$$

In just the same way we find the column maxima decrease with n. Therefore, both $m_j(n)$ and $M_j(n)$ have limits as $n \to \infty$. We must still show, however, that these two limits are the same.

To see this we estimate a little more carefully and we use (for the first time) the assumption that $W_{ij} \geq \epsilon$. Suppose that the minimum $m_j(n)$ and the maximum $M_j(n-1)$ are attained when $i = i_0$ and $i = i_1$, respectively. Then

$$m_j(n) = W_{i_0 j}^{(n)} = \sum_k W_{i_0 k} W_{kj}^{(n-1)}$$

$$= \epsilon W_{i_1 j}^{(n-1)} + (W_{i_0 i_1} - \epsilon) W_{i_1 j}^{(n-1)} + \sum_{k \neq i_1} W_{i_0 k} W_{kj}^{(n-1)}$$

$$\geq \epsilon M_j(n-1) + (1-\epsilon) m_j(n-1). \tag{B.5}$$

In just the same way we find that

$$M_j(n) \leq \epsilon m_j(n-1) + (1-\epsilon) M_j(n-1). \tag{B.6}$$

Subtracting (5) from (6) yields

$$M_j(n) - m_j(n) \leq (1-2\epsilon)[M_j(n-1) - m_j(n-1)], \tag{B.7}$$

so that

$$M_j(n) - m_j(n) \leqslant (1 - 2\epsilon)^n \, M \, [M_j(1) - m_j(1)]. \tag{B.8}$$

From Eq. (B.8) we conclude that $\lim_{n \to \infty}(M_j(n) - m_j(n)) = 0$.

Suppose we choose $m > 1$, then we know in any case that

$$\lim_{n \to \infty} W^{(n \cdot m)} = \Pi, \tag{B.9}$$

since the matrix $W^{(m)}$ falls into the case already treated. For any $k = 1, 2,..., m - 1$ we have

$$\lim_{n \to \infty} W^{(n \cdot m + k)} = \lim_{n \to \infty} W^{(k)} W^{(n \cdot m)} = W^{(k)} \Pi. \tag{B.10}$$

However, since $W^{(k)}$ has row sums equal to unity and Π has constant columns, $W^{(k)} \Pi$ is simply Π.

The transition matrix Π obviously satisfies the required conditions that $\Pi_{ij} > 0$ for all i and j, and $\sum_j \Pi_{ij} = 1$. The general form of this matrix is

$$\Pi = \begin{pmatrix} a & b & c & \cdots \\ a & b & c & \cdots \\ a & b & c & \cdots \\ & & \vdots & \end{pmatrix}, \tag{B.11}$$

where we identify each row as the vector

$$P^* = (a, b, c,...). \tag{B.12}$$

It immediately follows that P^* automatically satisfies

$$\sum_j P_j^* = 1, \tag{B.13}$$

and

$$P_j^* > 0 \qquad \text{for all } j. \tag{B.14}$$

We can interpret P^* as the set of equilibrium probabilities which describe our system in the limit $n \to \infty$. Extending this discussion to a continuous state space is an easy matter which we leave as an exercise.

APPENDIX C: DIAGONALIZATION OF THE HARMONIC OSCILLATOR TRANSFER MATRIX

The harmonic oscillator is, of course, an exactly solvable quantum system. This mqkes it a nice testing ground for our Monte Carlo techniques. In this appendix we give the exact solution to the oscillator path integral when the time lattice is in place.

By keeping all terms in the lattice spacing, we obtain expressions that can be directly compared with the Monte Carlo results at finite a.

The integral we wish to evaluate is

$$Z = \int \prod_{i=1}^{N} dx_i \exp\left(-\sum_{j=1}^{N} a \left[\frac{1}{2}\left(\frac{x_{j+1} - x_j}{a}\right)^2 + \frac{1}{2}\mu^2 x_j^2\right]\right). \tag{C.1}$$

Periodic boundary conditions $x_{n+1} = x_1$ are imposed and m_0 of Eq. (4.3) has been set to unity. From the functional integral point of view, this can be evaluated by noting that the action is a quadratic form and therefore the integral is Gaussian. A Fourier transform will make the quadratic form diagonal and the integral becomes trivial. In this appendix, however, we will be somewhat less conventional and evaluate Eq. (C.1) using operator techniques to diagonalize the transfer matrix.

Define the operator T by its matrix elements between position eigenstates

$$\langle x' \mid T \mid x \rangle = \exp\left(-\frac{1}{2a}(x' - x)^2 - \frac{u^2 a}{4}(x^2 + x'^2)\right). \tag{C.2}$$

The path integral for Z follows from inserting the completeness expression

$$1 = \mid x \rangle\langle x \mid \tag{C.3}$$

into the formula [11]

$$Z = \text{Tr}(T^N). \tag{C.4}$$

Here the trace is over the physical Hilbert space; for any operator A we define

$$\text{Tr}\, A = \int dx \langle x \mid A \mid x \rangle. \tag{C.5}$$

Using the fact that the canonical momentum generates translations

$$[p, x] = -i, \tag{C.6}$$

$$e^{-ip\Delta} \mid x \rangle = \mid x + \Delta \rangle, \tag{C.7}$$

we can obtain an expression for T in terms of the operators p and x

$$T = \int d\Delta\; e^{-(u^2 a/4)x^2} e^{-ip\omega} e^{-(1/2a)\omega^2} e^{-(u^2 a/4)p^2}. \tag{C.8}$$

The integral over Δ is Gaussian and yields

$$T = \sqrt{2\pi a}\; e^{-(u^2 a/4)x^2} e^{-(a/2)p^2} e^{-(u^2 a/4)x^2}. \tag{C.9}$$

Note that combining the exponents and dropping a^2 terms gives the exponentiated

harmonic oscillator Hamiltonian. Here, however, we will diagonalize Eq. (C.9) exactly, keeping all powers of a.

Using the commutator (C.6) we obtain

$$xT = T\left[\left(1 + \frac{a^2\mu^2}{2}\right)x - iap\right],\tag{C.10}$$

$$pT = T\left[\left(1 + \frac{a^2\mu^2}{2}\right)p + ia\mu^2\left(1 + \frac{a^2\mu^2}{4}\right)x\right].\tag{C.11}$$

Repeated use of these relations gives the remarkable result

$$\left[p^2 + \mu^2\left(1 + \frac{a^2\mu^2}{4}\right)x^2, T\right] = 0.\tag{C.12}$$

Thus T is diagonalized by the eigenstates of the simple harmonic oscillator Hamiltonian

$$H = \tfrac{1}{2}p^2 + \tfrac{1}{2}\omega^2 x^2,\tag{C.13}$$

where

$$\omega^2 = \mu^2\left(1 + \frac{a^2\mu^2}{4}\right).\tag{C.14}$$

Define the ladder operators

$$a = \frac{1}{\sqrt{2\omega}}(p - i\omega x),\tag{C.15}$$

$$a^+ = \frac{1}{\sqrt{2\omega}}(p + i\omega x).\tag{C.16}$$

We have

$$H = (a^+a + \tfrac{1}{2})\omega.\tag{C.17}$$

The desired eigenstates satisfy

$$a\,|\,0\rangle = 0,\tag{C.18}$$

$$(a^+)^n\,|\,0\rangle = |\,n\rangle,\tag{C.19}$$

$$\langle n\,|\,n\rangle = n!\tag{C.20}$$

Again using Eqs. (C.10) and (C.11) we obtain

$$aT = Ta\left(1 + \frac{a^2\mu^2}{2} - a\mu\left(1 + \frac{a^2\mu^2}{4}\right)^{1/2}\right).\tag{C.21}$$

As the states $|\,n\rangle$ diagonalize T

$$T\,|\,n\rangle = \lambda_n\,|\,n\rangle.\tag{C.22}$$

Equation (C.21) gives

$$\frac{\lambda_n}{\lambda_{n-1}} = 1 + \frac{a^2\mu^2}{2} - a\mu \left(1 + \frac{a^2\mu^2}{4}\right)^{1/2} = R, \tag{C.23}$$

where this defines R. Thus we conclude

$$T = \sqrt{2\pi a}\, K R^{(H/\omega)}, \tag{C.24}$$

where K is a normalization constant. To find K take the trace of T

$$\frac{1}{\sqrt{2\pi a}} \operatorname{Tr} T = K \sum_{n=0}^{\infty} R^{n+1/2} = \frac{K}{a\mu}$$

$$= \int \frac{dp\, dx}{2\pi} e^{-\mu^2 a x^2/2} e^{-a p^2/2} = \frac{1}{au}. \tag{C.25}$$

Thus $K = 1$ and we have the final result for T

$$T = \sqrt{2\pi a}\, R^{(H/\omega)} \tag{C.26}$$

The exact path integral is now easily evaluated

$$Z = (2\pi a R)^{N/2} \frac{1}{1 - R^N}. \tag{C.27}$$

Correlation functions follow simply from the representation

$$\langle x_i x_{i+j} \rangle = \frac{1}{Z} \operatorname{Tr}(x T^j x T^{N-j})$$

$$= \frac{1}{2\omega(1 - R^n)} (R^j + R^{N-j}). \tag{C.28}$$

Note that this equation includes all finite volume as well as finite spacing effects. Going to $j = 0$ gives

$$\langle x^2 \rangle = \frac{1}{2\mu(1 + a^2\mu^2/4)^{1/2}} \left(\frac{1 + R^N}{1 - R^N}\right). \tag{C.29}$$

The ground-state wavefunction is

$$\langle x \mid 0 \rangle = \left(\frac{\omega}{\pi}\right)^{1/4} \exp\left(-\frac{1}{2}\omega x^2\right). \tag{C.30}$$

The relation between ω and μ gives the numerical factors in Eq. (4.16).

REFERENCES

1. M. CREUTZ, L. JACOBS, AND C. REBBI, *Phys. Rev. Lett.* **42** (1979), 1390; *Phys. Rev. D* **20** (1979), 1915.
2. M. CREUTZ, *Phys. Rev. Lett.* **43** (1979), 533; BNL preprint No. 26847 (1979); K. G. WILSON, Cornell preprint (1979), G. BHANOT AND B. FREEDMAN, BNL preprint No. 27509 (1980), S. SHENKER AND J. TOBOCHNIK, Cornell preprint MSC No. 4243 (1980), G. A. JONGEWARD, J. D. STACK, AND C. JAYAPRAKASH, *Phys. Rev. D* **21** (1980), 3360.
3. R. P. FEYNMAN AND A. R. HIBBS, "Quantum Mechanics and Path Integrals," McGraw–Hill, New York, 1965.
4. A real time approach to evaluating the Feynman integral has been studied by G. Scher, M. Smith, and M. Baranger, MIT preprint No. 864 (1980).
5. N. METROPOLIS, A. ROSENBLUTH, M. ROSENBLUTH, A. TELLER, AND E. TELLER, *J. Chem. Phys.* **21** (1953), 1087; for a review of Monte Carlo methods applied to spin systems see K. Binder, *in* "Phase Transitions and Critical Phenomena" (C. Domb and M. S. Green, Eds.), Vol. 5B, Academic Press, New York, 1976.
6. For a survey of the mathematical theory of stochastic processes, see J. Lamperti, "Stochastic Processes," Applied Mathematical Sciences, Vol. 23, Springer-Verlag, Berlin/New York, 1977.
7. C.-P. YANG, Proceedings of Symposia in Applied Mathematics, Vol. XV, Amer. Math. Soc., Providence, R.I., 1963.
8. S. COLEMAN, "The Uses of Instantons," Lectures delivered at the 1977 International School of Subnuclear Physics, Ettore Majorana.
9. R. BLANKENBECLER, T. DEGRAND, AND R. L. SUGAR, *Phys. Rev. D* **21** (1980), 1055.
10. For a review of the effective potential, See B. ZUMINO, "1970 Brandeis Univ. Summer Institute in Theoretical Physics" (S. Deser, Ed.), Vol. 2, MIT Press, Cambridge.
11. M. CREUTZ, *Phys. Rev. D* **15** (1977), 1128; M. LUSCHER, *Comm. Math. Phys.* **54** (1977), 283; J. KOGUT, *Rev. Mod. Phys.* **51**, No. 4 (1979), 659.
12. B. LEE, *in* "Renormalization and Invariance in Quantum Field Theory," NASI series, Vol. B5 (E. R. Caianiello, Ed.), Plenum, New York, 1973.